32nd Congress
of the International Council
of the Aeronautical Sciences
September 6-10, 2021
Pudong Shangri-La, Shanghai, China

PASSIVE FLEXIBLE WINGTIP AREA FOR IMPROVING AIRLINERS CRUISE EFFICIENCY AND GUST ALLEVIATION

Gueraiche Djahid[1], Popov Sergey[2], Guelailia Ahmed[3]

[1, 2] Moscow Aviation Institute

[3] Center of Satellite Development, Space mechanical research development, Oran, Algeria

Abstract

Presented is a computational study of the potential benefits of using passive aeroelastic deformation of a high aspect ratio wing, with a flexible wingtip area, to both enhance the aircraft aerodynamic performance at transonic cruise conditions and alleviate gust loads. Preliminary results of CFD simulations based on NASA Common Research Model showed that the passively deformed wingtips alter significantly the local flow field near the wingtip area in the same way curved winglets do. Unlike curved winglets with a fixed geometry, a flexible wingtip section allows passive adjustment of its curvature proportionally to the aerodynamic loading conditions: at small angles attack during cruise, a less deformed configuration allows a higher lift-to-drag ratio and a better use of the available wing span. At higher angles of attack during take-off, climb and landing, a more curved configuration delays flow separation and stall onset on the outermost sections of the wing, thus allowing faster rates-of-climb at higher angles of attack and lower landing speeds to be achieved. Also, given a deflected wingtip section has a smaller local lift coefficient, this eliminates the need for a wing washout and allows gust alleviation, where dynamic load-proportional bending deflections compensate for sudden changes in dynamic pressure.

Keywords: wingtip area, aeroelasticity, inflected wing, fuel efficiency, gust alleviation.

1. Flexible wing concept: background research

Passenger airliner aerodynamics is one of the most conservative areas of aircraft design, where subsonic wing-and-tube layout experienced little changes since its introduction, becoming a true ‘common sense’ solution. NASA “N+3” vision foresees the subsonic wing-tube domination till at least 2030 prospective, where a lightweight aeroelastically tailored wing structure represents one of the most promising areas of research, that may have a near-future impact [1]. With a generally unchanging aerodynamic layout of transport aircraft, great leaps in material technology and elaboration of functionally graded materials with controllable anisotropy, allowed unprecedented opportunities for flexible wing configurations to be implemented. In a near-future prospective, these could allow to both passively and actively drive the wing shape and achieve an optimal geometry at different flight conditions.

Whilst aircraft structural design typically implies sufficient rigidity for safely handling the design flight loads, flutter and other aeroelastic phenomena, wide application of carbon laminates on recent airliners demonstrated the operational feasibility of high aspect ratio wings with unprecedented flexibility. Under loads, such wings are allowed to experience significant aeroelastic displacements without compromising the structural integrity. Given high aspect ratios are always key to low induced drag, pushing the boundaries of current aerodynamic performance is not possible without further increasing AR. Values already achieved by today’s wings are so large, that further increases in AR cannot be achieved without allowing significant aeroelastic displacements and/or the need for an additional supporting structure, e.g. the truss-braced wing, which is also a primary candidate concept for a near term impact on commercial aviation. Most notably the NASA-Boeing project SUGAR Volt with a projected aspect ratio of 19.5, which is nearly double the AR of current airliners [2]. Due to structural and aerodynamic constraints enforced by the truss, the flight Mach numbers are limited to low subsonic M~0.7. Therefore, cantilever solutions such as non-planar flexible wings hold a better promise for transonic cruise capability.

Despite the bird-inspired beginnings of flight and even the first powered flight of the Wright Flyer which implied indeed a morphing wing that warped for roll control, morphing research is relatively new in wing aerodynamics. Although multiple feasible enough concepts have been developed and some even passed flight testing [3], there is still a long way for flexible morphing wings to get implemented into operational aircraft. Among other issues hindering their certification, the most important are: reliability, flutter and other aeroelastic considerations as well as fatigue, maintenance and long term durability of flexible materials and structures. Soon after the Wright Flyer flight, aircraft designers were subsequently quick to replace the concept with more reliable, rigid control surfaces with mechanical joints. With increasing flight speeds, flutter margins have narrowed significantly and the concept of flexible wings has long fell out of favor, until composite materials gradually replaced aviation metals in recent decades. Implementation in primary structural elements of carbon-fiber reinforced plastics (CFRP) with significantly larger elasticity modulus than aluminum alloys is driving a new wave of flexibility in the design of lifting surfaces. Attempts include the developed in 2005 NASA Boeing X-53 with active aeroelastic wing [4] that uses active leading and trailing edge flaps to passively drive wing twist, which in return produces roll moments and controls the aircraft total lift. More recently, Airbus engineers flight-tested the “AlbatrossOne”, a model based on A321 equipped with movable wing tip sections almost a third of the wing span, hanging on semi-aeroelastic hinges. The concept is to use semi-passive, freely-flapping wing tips to reduce drag by increasing the aspect ratio with less structural weight penalties, given the relieved effect of wind gusts and turbulence [5]. To date, research and development is still in progress. A non-aviation project, which is of a particular interest to the topic is the attempted by Glenn et al. optimization of a Formula One rear wing for minimum induced drag at high speeds while maintaining sufficient aerodynamic down force at low speed turns [6]. The optimization was performed using lamination parameters of the wing panels for aeroelastic tailoring through bending-torsion coupling. The bended wing has a minimum angle of attack at high velocities, and therefore minimum drag. While at low speeds, high angles of attack due to torsional twist lead to maximum force and traction.

This paper represents a contribution towards flexible wing research, focusing on identifying local geometric and flow field parameters of the deflected wingtip area, and their dependency on the local bending-torsional stiffness of the wing structure. The local flow field is first explored through visualized results of CFD experiments, demonstrating, on a qualitative level, the aerodynamic feasibility of the concept and evaluating local values of flow field parameters. Fluid-structural experiments proved the structural benefits of the flexible wingtip, as compared to the baseline “rigid” wing of CRM model.

2. Materials and Methods

2.1. Concept exploration

In order to analyze the aeroelastic performance of an airliner wing with a flexible wingtip area, computational experiments have been carried out using NASA Common Research Model (CRM) as a baseline airliner configuration, which represents a conventional cruise configuration with a small static deflection of the wing cantilever. Fluid-structure interaction is computed in ANSYS Workbench environment using Fluent for computational fluid dynamics (CFD) and ANSYS Mechanical for structural simulations.

2.1.1 CFD model

A non-structured mesh of approximately 20 million tetrahedral cells has been generated using ANSYS Meshing and exported to Fluent to simulate the flow field near CRM model at cruise conditions of M=0.85 and an altitude of H=11km, Re=5 x 10^6. The mesh included 15 layers of a structured prismatic sub-mesh for boundary layer resolution. Mesh fragments are presented in figure 1 together with values of wall Y+ parameter on the main lifting surface of CRM model. Based on similar external aerodynamics computational results on DLR-F4 at similar Mach and Reynolds numbers and using a similar mesh [7], the SST standard k-ω turbulence model has been chosen and the energy equation included to account for compressibility. Preliminary validation was performed by comparison with results of wind tunnel tests in the “NASA Langley NTF” and “NASA Ames 11-Ft TWT” wind tunnels [8]. Given in Figure 2 are plots of lift and drag coefficients, where a very high accuracy of the CFD model is notable in predicting C_L values, especially the linear part of the lift curve, which almost fully corresponds to the wind tunnel test results. Flow separation onset at high angles of attack, larger than $\alpha=6^o$, causes discrepancies with acceptable errors up until $\alpha=8^o$. The computed drag coefficients differ slightly from the wind tunnel experiments, where overestimated values of C_d are noticeable at small angles of attack. Overall, the CFD model demonstrated a good fidelity and is suitable for further investigations on CRM geometry.

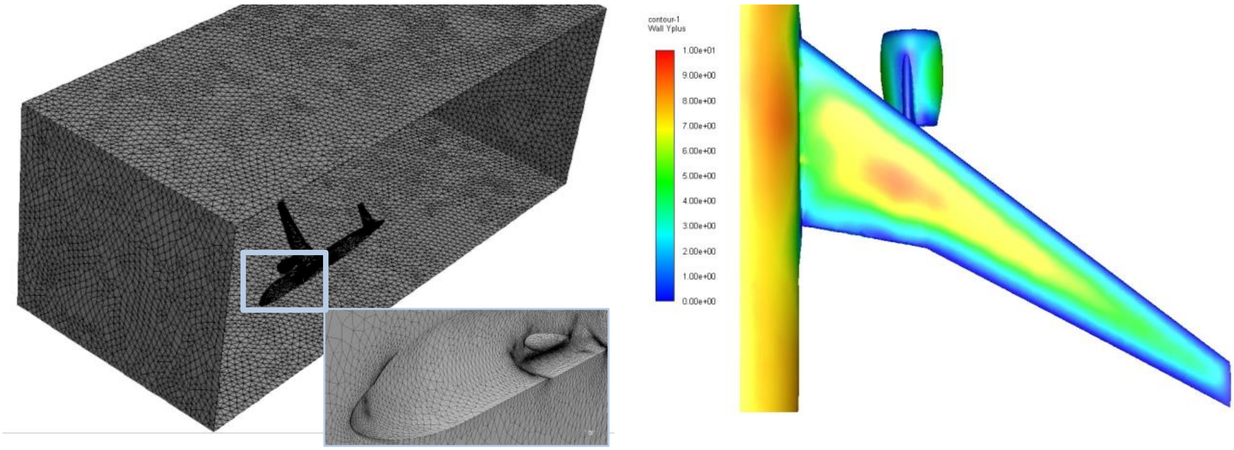

Figure 1 – A fragment of the computational domain mesh and Wall Y+ values on the surface of CRM model.

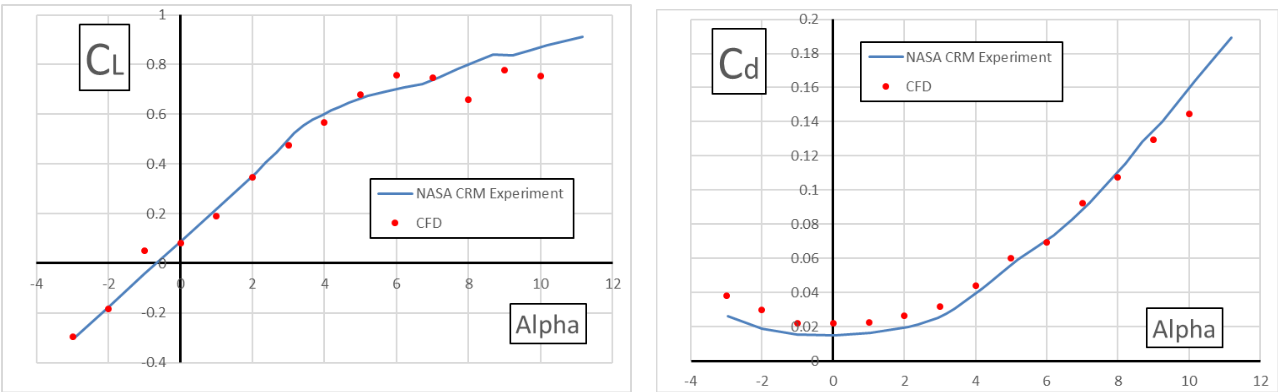

Figure 2 – Validation of the CFD model: lift and drag coefficients dependences on the angle of attack, obtained from computational model and wind tunnel experiments.

2.1.2 Structural model

Pressure distribution obtained from the CFD model is exported along the geometry to ANSYS Mechanical for aeroelastic simulations. The CRM structural model is made of a hypothetic anisotropic material with an initial spanwise distribution of the wing bending stiffness $EI(z)=S^{ini.}(z)$, which is, by concept definition, assumed to enable maximum rigidity only near the wing root and engine mount, due to significant local loads. While from the Yehudi break of the wing trailing edge, gradually reducing stiffness towards the wingtip area allows maximum wingtip displacements to be achieved. This results in a non-planar inflected shape with aerodynamic loading shifted towards the wing root. Based on optimal winglet shapes investigated in [7], including curved winglets which geometry is much similar to the inflected part of the wing, the initial stiffness distribution is defined as an exponential, monotonic decreasing function: $S^{ini.}(z)=b^z$, where $0<b<1$. In this first phase, the value of *b* is found by trial and error such, to produce a deflected wing shape, as close as possible to an elliptic winglet, which has been proved to be optimal for cruise conditions from the winglet study [7].

The engine weight is imitated by a static down force $W_{eng.}$, applied to the engine nacelle. $W_{eng.}$ is estimated given its ratio to the hypothetical aircraft weight, equal to CRM lift force at cruise with g=1: $W_{aircraft} = L_{CRM}$ ~ 1312 kg. For twin jet airliners, engines represent ~8% of $W_{aircraft}$, hence a single engine for CRM weighs $W_{eng.\_CRM}$ ~ 52.5 kg. The fuselage and tail of CRM are defined as a fixed support, thus imitating aeroelastic behavior of the wing at *g=1* condition, where fuselage and engine weights are balanced by the lift force. A high resolution is ensured for the structural mesh of the wing flexible part, from the trailing edge break to the wingtip. The structural model and mesh are illustrated in Figure 3.

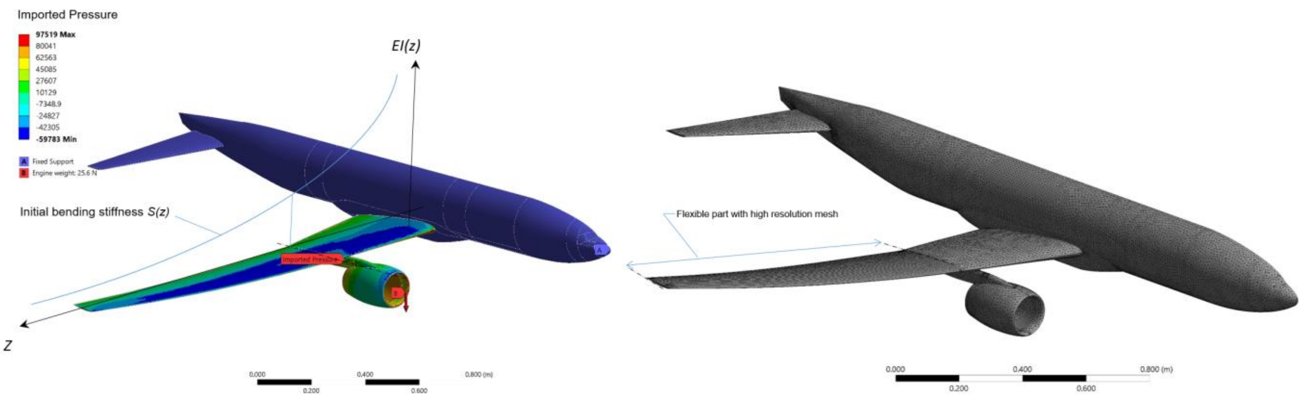

Figure 3 – CRM structural model and mesh used to analyze the wing aeroelasticity.

2.1.3 Simulation results

Flow field visualization at a moderately high angle of attack α=4° of the flexible wing shows a decrease in induced drag as compared to the “rigid” wing, and flow field patterns near the lifted tip, are much similar to that of a wingletted wing. Induced drag magnitude can be qualitatively estimated from Figure 4 below, where the rigid configuration features an important wingtip vortex with a low pressure in its core, as shown by the magnitude (velocity values) and color (local pressure) of velocity vectors projection on the Treftz plane behind the wing tip (Figure 4 a). The tip vortex is significantly altered by the inflected wingtip, leading to a less intensity and a higher pressure behind the wing, hence less induced drag (Figure 4 b). Pressure distribution on the upper surface of the wing at Figure 4 shows that, the inflected state shifts the aerodynamic loading towards the wing root. This is indicated by the lower pressure values (a darker blue) along the top surface of the rigid wing (a), while a lighter blue color towards the lifted wing tip to the right indicates lower local loadings (b).

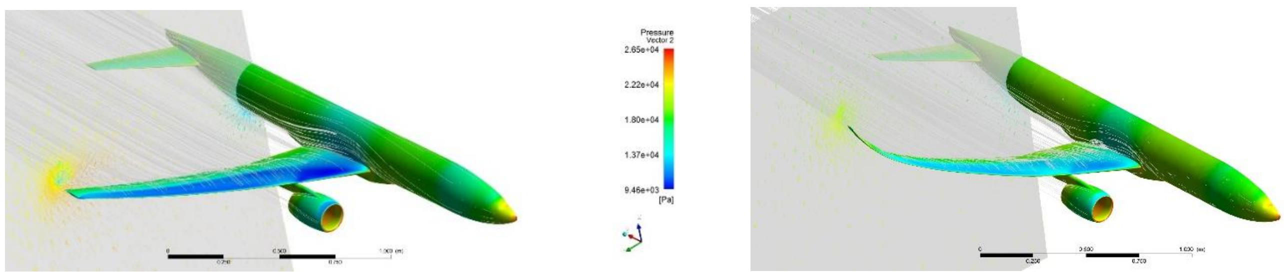

Figure 4 – Flow field visualization at cruise conditions for CRM initial rigid model and comparison with the flexible wing configuration.

A closer look at the tip flow field reveals a negative angle attack on the outermost sections of the lifted tip. This is illustrated by velocity vectors in section planes in Figure 5 (b) and surface pressure in Figure 5 (b), where low pressure, blue color is observed beneath the lifted tip. This is caused by the bending-torsion coupling of the swept back wing, where significant bending deflections lead to a nose-down twist of the tip. This leads to a negative lift on the tip, which stops further bending deflections of the wing cantilever and the deformed wing converges to its final curved shape. By increasing the torsional stiffness of tip sections, the onset of negative tip angles of attack can be delayed, allowing further bending deflections of the wing cantilever with higher angles of attack, leading to a more curved wing shape. This pattern can be observed in Figure 6 a, where despite a very high flight α=6°, increasing local torsional stiffness by 20% has delayed the onset of negative tip angles of attack, while in Figure 6 b, at already α=3°, negative lift is observed at the tip due to low local torsional stiffness.

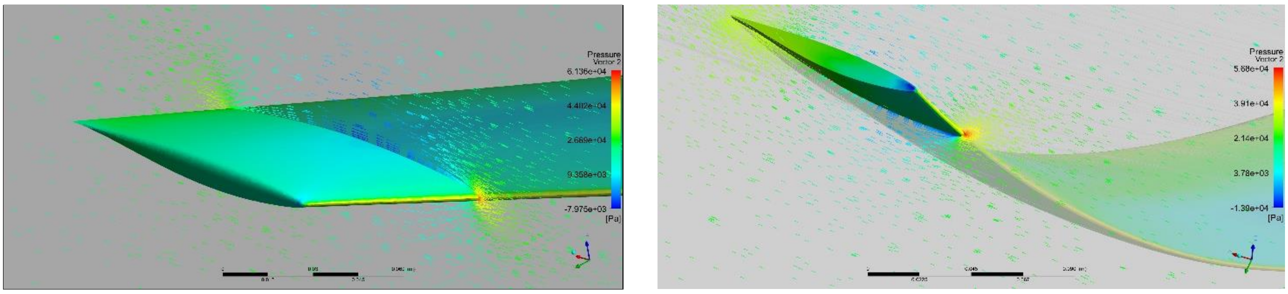

(**a**) (**b**)

Figure 5 – Flow field visualization at cruise conditions for CRM initial rigid model and comparison with the flexible wing configuration.

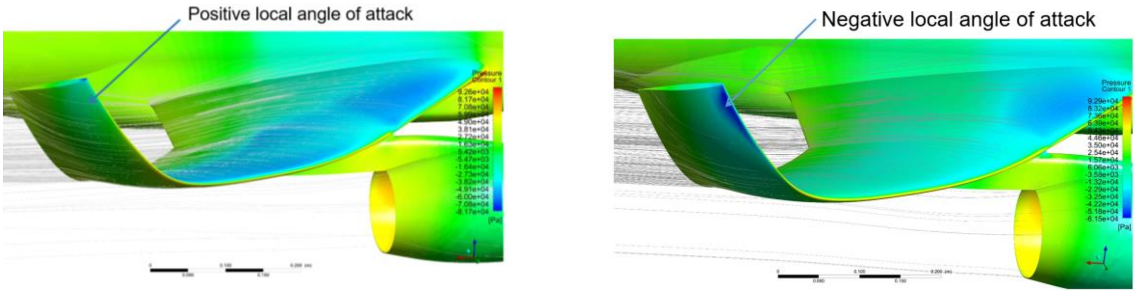

(**a**) (**b**)

Figure 6. Effect of high (a) and low (b) torsional stiffness on local angles of attack at CRM flexible wing tip.

2.1.4 Gust load alleviation using flexible wingtips

As illustrated by the plot in Figure 6 below, bending-torsion coupling leads to a general decrease in the total lift generated by the inflected wing as compared to the baseline straight wing. The decrease in CL is the more significant the higher the dynamic pressure and/or the higher the angle of attack, given higher angles of attack and dynamic pressures cause further tip deflections and less loading on tip sections.

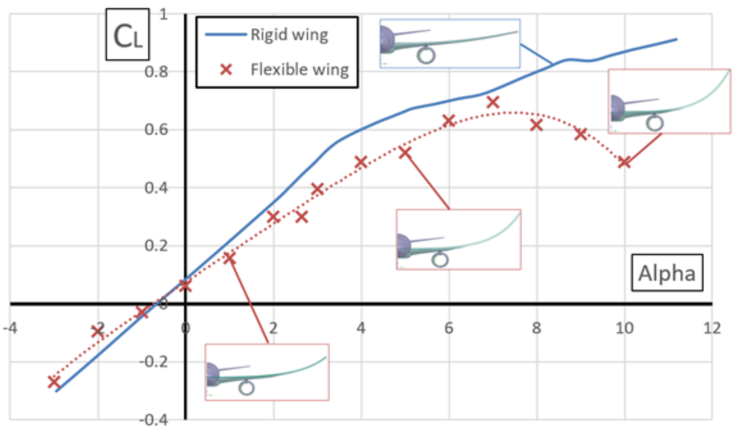

Figure 6 – Lift coefficient by angle of attack of CRM rigid and flexible wing configurations.

The static gust load of 2.5g's, which corresponds to the ultimate certification load for this type of aircraft, has been modeled by a "fixed support" constraint for the fuselage, while increasing dynamic pressures and/or the angle of attack until the lift exceeded the hypothetical weight of the aircraft, Waircraft, by 2.5 times. As mentioned earlier, at cruise conditions the aircraft weight should be equal to the lift generated by CRM wing at cruise angle of attack α=3º: $W_{aircraft} = L_{CRM}$ ~ 1312 kg. Therefore, the required lift to produce a 2.5 g-load is equal to: L2.5g = 2.5 Waircraft ~ 3280 kg. The flight conditions on CRM, required to generate this lift are achievable for instance at the maximum lift coefficient C_{L_max} ~ 0.8 (α~6º), and an air density altitude of H ~ 5 km. Fluid-structure simulations showed that the kinetic energy of the gust at these conditions is effectively absorbed by tip deflections and not transformed to the wing root, hence a much less stressed root is observed, see Figure 7 below. Time-dependent dynamic gust loads are planned to be tested in future experiments.

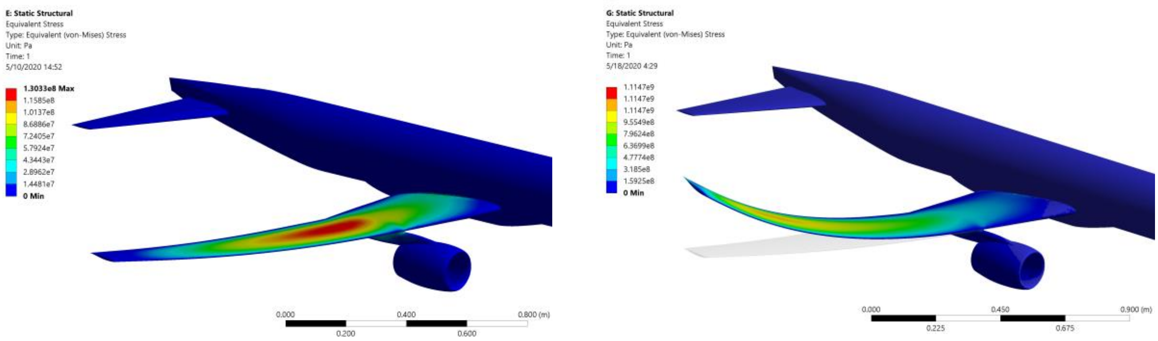

(**a**) (**b**)

Figure 7. Equivalent von-Mises stress at 2.5 g's for CRM rigid wing (a) and comparison with the flexible wing configuration (b).

Increases in dynamic pressure that otherwise would have led to proportional increases in the aircraft total lift force, in the case of a flexible wingtip given at higher loading conditions the deflected wing possesses 15 – 20% less lift (plot at Figure 6), the total lift force remains closer to its initial values. Thus, similar to a suspension system for a road vehicle, flexible tips passively absorb fluctuations of dynamic pressure, leading to a virtually constant lift force and a smoother ride in turbulent atmospheres. In order for the values of lift increase due to dynamic pressure fluctuations to be passively balanced by lift losses due to tip deflections without falling below the lift required for level flight, the wing bending-torsional stiffness distribution has to be carefully tailored. Using the computational approach, the quest for an optimal stiffness distribution for both cruise and gust conditions follows the routine in Figure 8, where the stiffness distribution is constantly updated in a closed two-way FSI cycle until the wing shape converges to an optimal curvilinear shape. Given spanwise stiffness in both bending and torsional axes has to be optimized along with the wing geometry, this requires significant computational time and resources. An alternative analytic design methodology is presented in [9], which is aimed at identifying an initially optimized stiffness before starting the computational routine, using analysis of the dependency of local lift values on the wing curved shape, which in turn is a function of the local bending-torsional stiffness.

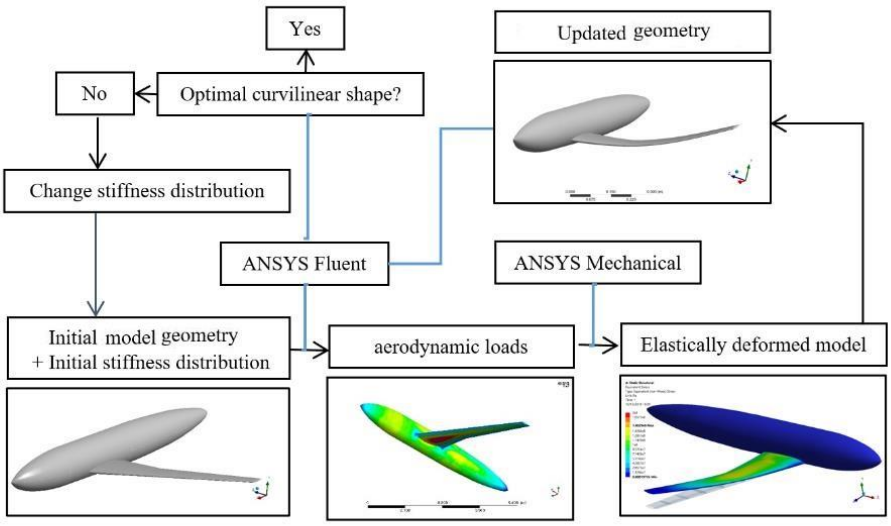

Figure 9 – Optimization routine for the wing spanwise stiffness distribution using two-way fluid-structure interaction experiments in ANSYS Workbench environment.

3. Discussion

Presented is a brief concept study of a high aspect ratio, aeroelastically tailored airliner wing with a near-future potential for replacing wingletted wings of current airliners. This wing concept exploits the aerodynamic benefits of winglets on a much larger portion of the flight envelope, given unlike winglets with a fixed geometry optimized solely for cruise efficiency, the flexible wing tips allow passive adaptation of their shape to match aerodynamic loading conditions. Thus, allowing a larger wing aspect ratio with less structural weight penalties. The passively deformed wing tips absorb the energy of gust loads, reducing or eliminating the need for complex active gust cancellation systems.

Analytic design methodologies, such as in [9] could be effectively used to correlate the tightly coupled aspects of flexible wing design: aerodynamic, structural and geometrical. This was achieved through mathematical parametrization of the inflected wing shape, then using parametrized functions to calculate local values of aerodynamic loading, which are dependent on local angles of attack. With a known aerodynamic loading distribution, cantilever beam theory can be effectively exploited to determine the required distribution of bending and torsional stiffnesses along the wing span, therefore reducing the computational time and resources required for higher fidelity optimization.

Practical realization of this concept is possible through the use of anisotropic composite materials with controllable stiffness distribution in different axes. Hence, a future research is required using a real composite material data and lamination parameters to get the precalculated bending-torsional stiffness distribution, that in turn will produce the desired optimal curvilinear wing at each flight regime and loading conditions. Other aeroelastic aspects should be taken into account, such as identifying the margins of flutter, divergence and aileron reverse. Constraints on the wing flexibility are also imposed by fatigue stress and determination of the maximum allowable number of loading cycles. Similar to springs and other elements of road vehicles suspension systems, flexible wing tips would probably require regular replacements.

3. Contact Author Email Address

Gueraiche Djahid: d.gueraiche@mai.ru

Popov Sergey: flowmech@mail.ru

Guelailia Ahmed: guelailia@yahoo.fr

4. Copyright Statement

References

[1] Sam Bruner, Scott Baber, Chris Harris et al. *NASA N+3 Subsonic Fixed Wing Silent Efficient Low-Emissions Commercial Transport (SELECT) Vehicle Study*. Revision A, Tufts University, Medford, Massachusetts, 2010.

[2] Marty K Bradley and Christopher K Droney *Subsonic Ultra Green Aircraft Research: Phase II – Volume II – Hybrid Electric Design Exploration*. NASA/CR–2015-218704/Volume II, NASA report, April 2015.

[3] Joel A. Hetrick, Russell F. Osborn et al. Flight Testing of Mission Adaptive Compliant Wing. 48th AIAA/ASME/ASCE/AHS/ASC Structures, Structural Dynamics, and Materials Conference, Honolulu, Hawaii, 15th 23 - 26 April 2007.

[4] Ed Pendleton, Pete Flick et al. The X-53 A summary of the active aeroelastic wing flight research program. 48th AIAA/ASME/ASCE/AHS/ASC Structures, Structural Dynamics, and Materials Conference, Honolulu, Hawaii, 15th 23 - 26 April 2007.

[5] Thomas Wilson, Andrea Castrichini. Small scale flying demonstration of semi aeroelastic hinged wing tips. International Forum on Aeroelasticity and Structural Dynamics IFASD 2019, Savannah, Georgia, USA. 9-13 June 2019

[6] Thuwis, G.A.A., De Breuker, R., Abdalla, M.M. et al. Aeroelastic tailoring using lamination parameters. Struct Multidisc Optim 41, 637–646 (2010).

[7] Gueraiche D, Popov S. Winglet Geometry Impact on DLR-F4 Aerodynamics and an Analysis of a Hyperbolic Winglet Concept. *Aerospace,* Vol. 4, No. 4:60, 2017.

[8] Melissa B Rivers, Ashley D. Experimental Investigations of the NASA Common Research Model in the NASA Langley National Transonic Facility and NASA Ames 11-Ft Transonic Wind Tunnel (Invited). *49th AIAA Aerospace Sciences Meeting including the New Horizons Forum and Aerospace Exposition*, Orlando, Florida, USA, AIAA 2011-1126, 4 - 7 January 2011.

[9] D Gueraiche et al. Analytic design methodology for flexible wing parametrization and spanwise load estimation. 2021 IOP Conference Series: Mater. Sci. Eng. 1047 012056